BIOCHEMICAL PHARMACOLOGY 75 (2008) 1659–1669

available at www.sciencedirect.com

ScienceDirect

journal homepage: www.elsevier.com/locate/biochempharm

Role of proline 1150 in functional interactions between the membrane spanning domains and nucleotide binding domains of the MRP1 (ABCC1) transporter

Isabelle J. Létourneau, Akio Nakajima, Roger G. Deeley, Susan P.C. Cole *

Department of Pharmacology & Toxicology, Division of Cancer Biology & Genetics, Cancer Research Institute, Queen's University, Kingston, Ontario, Canada K7L 3N6

ARTICLE INFO

Article history:
Received 5 December 2007
Accepted 22 January 2008

Keywords:
MRP1
Organic anion transport
ATP-binding and hydrolysis
Active transport
ATP-binding cassette

ABSTRACT

The ATP-binding cassette multidrug resistance protein 1 (MRP1) mediates ATP-dependent cellular efflux of drugs and organic anions. We previously described a mutant, MRP1-Pro1150Ala, which exhibits selectively increased estradiol glucuronide ($E_2$17βG) and methotrexate transport as well as altered interactions with ATP. We have now further explored the functional importance of MRP1-Pro^{1150} at the interface of transmembrane helix 15 and cytoplasmic loop 7 (CL7) by replacing it with Gly, Ile, Leu and Val. All four mutants exhibited a phenotype similar to MRP1-Pro1150Ala with respect to organic anion transport and [γ^{32}P]8N_3ATP photolabeling. They also displayed very low levels of substrate-independent vanadate-induced trapping of [α^{32}P]8N_3ADP. To better understand the relationship between the altered nucleotide interactions and transport activity of these mutants, [α^{32}P]8N_3ADP trapping experiments were performed under different conditions. Unlike leukotriene C_4, $E_2$17βG decreased [α^{32}P]8N_3ADP trapping by both wild-type and mutant MRP1. [α^{32}P]8N_3ADP trapping by MRP1-Pro1150Ala could be increased by using Ni^{2+} instead of Mg^{2+}, and by decreasing temperature; however, the transport properties of the mutant remained unchanged. We conclude that the reduced [α^{32}P]8N_3ADP trapping associated with loss of Pro^{1150}, or the presence of $E_2$17βG, is due to enhanced ADP release following ATP hydrolysis rather than a reduction in ATP hydrolysis itself. We hypothesize that loss of Pro^{1150} alters the role of CL7 as a coupling helix that mediates signaling between the nucleotide binding domains and some substrate binding sites in the membrane spanning domains of MRP1.

1. Introduction

Multidrug resistance protein 1 (MRP1, ABCC1) is a member of the ATP-binding cassette (ABC) superfamily of transmembrane proteins, subfamily C [1,2]. It was first identified in a multidrug resistant lung cancer cell line selected in doxorubicin and, by enhancing efflux, MRP1 can confer resistance to many anticancer agents including doxorubicin, vincristine, etoposide and mitoxantrone in an ATP-dependent manner [3–5]. Other substrates of MRP1 include a large number of conjugated and unconjugated organic anions, such as the GSH-conjugated leukotriene

* *Corresponding author*. Fax: +1 613 533 6830.
E-mail address: spc.cole@queensu.ca (Susan P.C. Cole).

Abbreviations: MRP, multidrug resistance protein; ABC, ATP-binding cassette; MSD, membrane spanning domain; NBD, nucleotide binding domain; LTC_4, leukotriene C_4; $E_2$17βG, 17β-estradiol 17β-D-glucuronide; CL, cytoplasmic loop; MTX, methotrexate; HEK, human embryonic kidney; TM, transmembrane; TSB, Tris–sucrose buffer; MAb, monoclonal antibody.

0006-2952/$ – see front matter © 2008 Elsevier Inc. All rights reserved.
doi:10.1016/j.bcp.2008.01.009

C_4 (LTC_4), the conjugated estrogen, estradiol 17β-glucuronide ($E_217\beta G$) and the antifolate methotrexate (MTX) [2,6–8].

MRP1 is composed of three membrane spanning domains (MSDs) containing 5, 6 and 6 transmembrane (TM) α-helices, respectively. In addition, two functionally non-equivalent nucleotide binding domains (NBDs) are responsible for the binding and hydrolysis of ATP which power the transport process [9]. The transporter is expressed ubiquitously throughout the body, except in the liver where it is usually not detectable. In polarized epithelial and endothelial cells, it is found mainly on basolateral membranes [1]. The murine ortholog of MRP1 has been demonstrated to be an *in vivo* mediator of LTC_4 efflux during inflammatory responses [10]. MRP1/Mrp1 also has an important role in protecting some normal tissues from the adverse effects of various toxicants and cytotoxic drugs [1].

We previously described a phenotypically complex MRP1 mutant in which a conserved proline residue, predicted to be at the beginning of cytoplasmic loop 7 (CL7) connecting TM15 to TM16, was replaced with alanine [11]. Compared to wild-type MRP1, the Pro1150Ala mutant displayed decreased levels of LTC_4, estrone sulfate, and GSH transport but substantially increased levels of $E_217\beta G$ and methotrexate (MTX) transport. The increased $E_217\beta G$ transport by MRP1-Pro1150Ala was associated with a 5-fold decrease in apparent $K_m(E_217\beta G)$ and 4-fold decrease in K_m(ATP) during $E_217\beta G$ transport. However, the apparent K_m(ATP) values for wild-type MRP1 and MRP1-Pro1150Ala were the same during LTC_4 transport.

The interaction of the MRP1-Pro1150Ala mutant with nucleotide was further investigated using the ^{32}P-labeled photoaffinity ligand $8N_3ATP$. The ability of a protein to trap $[\alpha^{32}P]8N_3ADP$ in the presence of sodium orthovanadate under conditions that permit ATP hydrolysis is often measured as an indicator of its ATPase activity, while $[\gamma^{32}P]8N_3ATP$ photolabeling under non-hydrolytic conditions is an indicator of its ATP-binding capacity [12]. In the case of MRP1-Pro1150Ala, vanadate-induced trapping of $[\alpha^{32}P]8N_3ADP$ was greatly diminished relative to wild-type MRP1, while photolabeling of this mutant with $[\gamma^{32}P]8N_3ATP$ under non-hydrolytic conditions was unchanged [11]. Taken together, these data suggested that Ala substitution of the conserved Pro^{1150} in MRP1 caused a substrate-selective effect on both the transport activity of MRP1 and its dependence on ATP, while at the same time having a substrate-independent effect on vanadate-induced trapping of ADP or ATPase activity. We recently showed that mutation of the proline residues in the MRP1 homologs MRP2 and MRP3 corresponding to MRP1-Pro^{1150} also resulted in changes in substrate specificity and ADP trapping indicating the function of this residue is largely conserved [13].

The objective of the present study was to explore further the functional role of Pro^{1150} in MRP1 by replacing it with four additional amino acids (Gly, Leu, Ile and Val) with different physicochemical properties. The resulting MRP1 mutants were characterized with respect to their substrate specificities and inhibitor sensitivities as well as their interactions with ATP.

2. Materials and methods

2.1. Reagents

[14,15,19,20-^{3}H]LTC_4 (158 Ci mmol^{-1}) and [6,7-^{3}H]$E_217\beta G$ (45 Ci mmol^{-1}) were purchased from PerkinElmer Life Sciences (Woodbridge, ON, Canada). [3′,5′,7′-^{3}H (*n*)]MTX sodium salt (33.5 Ci mmol^{-1}) was from Moravek Inc. (Brea, CA). LTC_4 was purchased from CalBiochem (San Diego, CA). AMP, ATP, $E_217\beta G$, S-decyl-GSH, GSH, sodium orthovanadate, diphenylcarbamyl chloride-treated trypsin and BAY u9773 were purchased from Sigma Chemical Co. (St. Louis, MO). Creatine kinase and creatine phosphate were obtained from Roche Diagnostic (Laval, QC, Canada). MTX sodium salt was purchased from Faulding (Vaudreuil, QC, Canada). $[\alpha^{32}P]8N_3ATP$ (12 Ci mmol^{-1}) and $[\gamma^{32}P]8N_3ATP$ (10.6 Ci mmol^{-1}) were purchased from Affinity Labeling Technologies Inc. (Lexington, KY). LY465803 was a gift from Eli Lilly (Indianapolis, IN) [14], and MK571 was purchased from Cayman Chemicals (Ann Arbor, MI). MAbs MRPm6 and MRPr1 were kind gifts from Drs. R.J. Scheper and G.L. Scheffer (Amsterdam, Netherlands).

2.2. Site-directed mutagenesis

The generation of the MRP1-Pro1150Ala mutant expression construct has been described previously [11]. Additional substitutions of Pro^{1150} in MRP1 were generated using the QuickChange Site-Directed Mutagenesis Kit (Stratagene, La Jolla, CA), and a template generated by subcloning a 2-kb XmaI fragment encoding amino acids 780–1440 from pcDNA3.1(−)$MRP1_k$ into pGEM-3Z. Mutagenic oligonucleotide primers were obtained from IDT Inc. (Coralville, IA). Mutagenesis was performed according to the manufacturer's instructions with the following sense primers (the substituted nucleotides causing the mutation are underlined; silent nucleotide substitutions added to introduce or disrupt a restriction site are in bold; other nucleotide substitutions are in lowercase typeface; and diagnostic restriction enzymes are indicated in parentheses): MRP1-Pro1150Gly (5′-G TCG GTC AGC CGG TC**g** GGG GTC TAT TCC C-3′) (BsrFI), MRP1-Pro1150Ile (5′-C AGC CGC TCC ATC GTC TA**C** TCC CAT TTC AAC-3′) (AccI), MRP1-Pro1150Leu (5′-CG GTC AGC CG**G** TCC CTC GTC TAC TCC CAT TTC-3′) (AccI) and MRP1-Pro1150Val (5′-CG GTC AGC CG**G** TCC GTG GTC TAT TCC C-3′) (RsrII). Following mutagenesis, the desired fragment was subcloned back into pcDNA3.1(−)$MRP1_k$ as a 1.3-kb Esp3I/EcoRI fragment, and the sequence fidelity verified (ACGT Corp., Toronto, ON, Canada).

2.3. Transfections in HEK293T cells and membrane vesicle preparation

Mutant or wild-type pcDNA3.1(−)$MRP1_k$ vectors were transfected into human embryonic kidney (HEK293T) cells seeded at approximately 18×10^6 cells per 150 mm plate. After 24 h, cells were transfected with 20 μg DNA using Lipofectamine™ 2000 (Invitrogen, Carlsbad, CA) according to the manufacturer's instructions. After 48 h, the HEK293T cells were collected and stored as cell pellets at −70 °C until needed. Membrane vesicles were prepared as described previously and stored at −70 °C until required [7].

2.4. Determination of MRP1 levels in transfected cells

Levels of MRP1 in the membrane vesicles were determined by immunoblot analysis using the human MRP1-specific murine MAb QCRL-1 (1:10,000) and a chemiluminescence detection system as described [15]. The films were analyzed by densitometry using Image J software (http://rsb.info.nih.gov/ij/).

2.5. Limited trypsin digestion of MRP1

Membrane vesicles (0.25 μg μl^{-1}) diluted in TSB were incubated with trypsin at trypsin:protein ratios ranging from 1:5000 to 1:1 for 15 min at 37 °C. Reactions were stopped by adding Laemmli buffer with protease inhibitors on ice and the samples loaded on a 4–20% gradient acrylamide gel (Pierce, Rockfort, IL) and immunoblotted. Full-length and tryptic fragments of MRP1 were detected by chemiluminescence detection assays using MAb MRPm6 (1:1000) which recognizes an epitope at the COOH-terminus and MAb MRPr1 (1:5000) which recognizes an epitope in the NH_2-proximal half of MRP1 [16].

2.6. MRP1-mediated transport of ^{3}H-labeled organic anions by membrane vesicles

ATP-dependent uptake of ^{3}H-labeled organic anion substrates by the MRP1-enriched membrane vesicles was measured using a rapid filtration technique in a 96-well plate format [7,17,13]. Typical reactions were carried out in triplicate in TSB in a final reaction volume of 30 μl and containing either $MgCl_2$ (10 mM) and AMP (2 mM) or $MgCl_2$ (10 mM), ATP (2 mM), creatine phosphate (10 mM) and creatine kinase (100 μg ml^{-1}). In some experiments, ATP was replaced by $8N_3$ATP.

Transport assays with modulators were carried out as described above in a final volume of 50 μl. A stock solution of MK571 was prepared in methanol, BAY u9773 and LY465803 were dissolved in DMSO, and S-decyl-GSH in 1N NH_4OH. The final concentration of vehicle never exceeded 1% of the final reaction volume. Membrane vesicles were preincubated with modulators for 15 min on ice before proceeding with the transport experiments.

Transport in the presence of AMP was subtracted from transport in the presence of ATP to determine ATP-dependent uptake and data were fitted to sigmoidal dose-response curves by non-linear regression analysis. The log IC_{50} values and IC_{50} values for the modulators were determined using GraphPad Prism 3.0 software. Statistical comparisons of the IC_{50} values for wild-type MRP1 and MRP1-Pro1150Ala were carried out using a paired Student *t*-test and considered significant when $p < 0.05$.

2.7. Photolabeling of MRP1 with [^{3}H]LTC_4 and [γ^{32}P]$8N_3$ATP

Membrane proteins were photolabeled with [^{3}H]LTC_4 as described previously [11]. Briefly, membrane vesicles (50 μg protein) were incubated with [^{3}H]LTC_4 (200 nM; 0.08–0.1 μCi) and 10 mM $MgCl_2$ in a final volume of 50 μl for 30 min at room temperature and then frozen in liquid nitrogen. When a substrate was included in the experiment, membrane vesicle proteins were incubated with the substrate for 30 min on ice before adding [^{3}H]LTC_4 and $MgCl_2$. After irradiation at 302 nm, radiolabeled proteins were resolved by SDS-PAGE. After drying, the gel was exposed to Bioflex MSI film (InterScience, Markham, ON, Canada) for 5 days at −70 °C. The films were analyzed by densitometry using Image J software as described above.

Membrane vesicle proteins were photolabeled with [γ^{32}P]$8N_3$ATP also as described previously [11]. Briefly, membrane vesicles (10 μg protein) were incubated with 5 mM $MgCl_2$ and 5 μM [γ^{32}P]$8N_3$ATP (1 μCi) in a final volume of 20 μl. After 5 min on ice, the samples were cross-linked at 302 nm, washed, and then solubilized in Laemmli buffer and subjected to SDS-PAGE. After drying, the gel was exposed to film for 2–12 h.

2.8. Vanadate-induced trapping of [α^{32}P]$8N_3$ADP by MRP1

MRP1-enriched membrane vesicles (10 μg protein) were incubated in TSB (20 μl) containing $MgCl_2$ (5 mM) or $NiCl_2$ (5 mM), with and without freshly prepared sodium orthovanadate (1 mM), [α^{32}P]$8N_3$ATP (5 μM, 1 μCi) for 15 min at 37 °C except where indicated. In some experiments, membrane vesicles were incubated with $E_2$17βG for 10 min on ice before adding the reaction mix containing the [α^{32}P]$8N_3$ATP. Reactions were terminated by the addition of ice-cold Tris–EGTA buffer, centrifuged, and membrane proteins resuspended before irradiating at 302 nm as before [11]. Membrane vesicles were then solubilized in Laemmli buffer, subjected to SDS-PAGE, and after drying, the gel was exposed to film for 12–24 h.

3. Results

3.1. Mutation of Pro^{1150} affects the trypsin sensitivity of MRP1

To determine whether the functional impact of the MRP1-Pro^{1150} mutation was associated with changes in MRP1 structure, limited trypsin digests of wild-type MRP1 and the MRP1-Pro1150Ala mutant were performed side-by-side and the fragments probed by immunoblotting with MAbs against the NH_2-proximal (N1, N3) (MAb MRPr1) and COOH-proximal (C1, C2) (MAb MRPm6) halves of MRP1 (Fig. 1A). As shown in Fig. 1B and C, the Pro1150Ala mutant was more resistant to trypsin digestion than wild-type MRP1 as evident from the persistence of the full-length protein at high trypsin:protein ratios. On the other hand, no significant differences were observed in the trypsin sensitivity of the initial COOH-proximal (C1) and NH_2-proximal (N1) fragments generated. Similar observations were made when chymotrypsin was used instead of trypsin (results not shown). Other mutants described below were not tested by limited trypsin digests.

3.2. Substitution of Pro^{1150} does not affect MRP1 expression in HEK293T cells

MRP1 was subjected to site-directed mutagenesis to create Gly, Ile, Leu and Val substitutions of Pro^{1150}. Immunoblots of the membrane vesicles prepared after transient expression in HEK293T cells revealed that none of the four mutations affected levels of MRP1 expression relative to wild-type MRP1

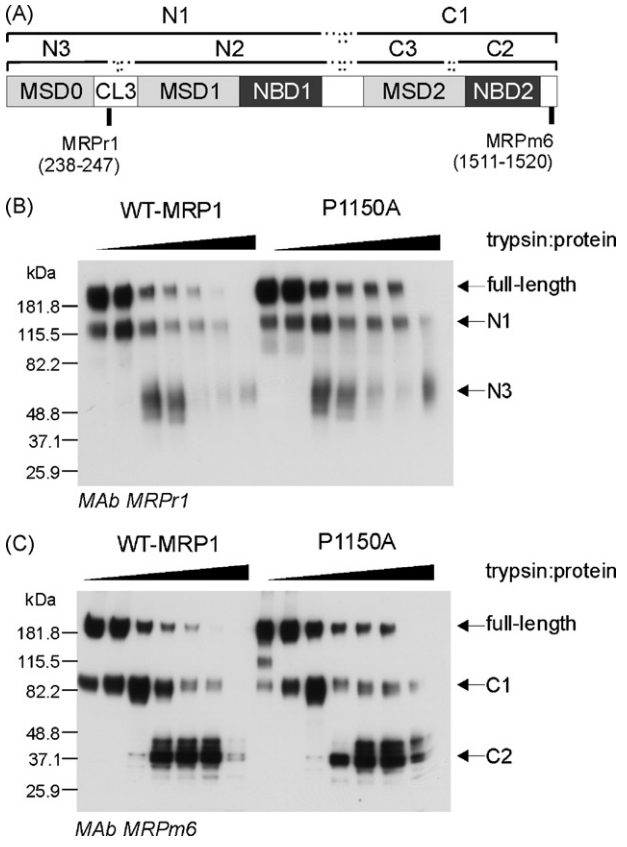

Fig. 1 – Limited trypsin digestion of wild-type MRP1 and Pro1150Ala mutant MRP1. (A) Shown is a schematic representation of the MRP1 protein with the sites of initial trypsin cleavage indicated, together with the approximate sizes of the resulting tryptic fragments (N1, N2, N3, C1, C2 and C3), and the epitopes detected by the MAbs used for immunoblotting [16]. (B and C) Membrane vesicle protein (2 μg per lane) was incubated at 37 °C with increasing concentrations of trypsin (trypsin:protein ratios 1:5000 to 1:1) as described in Section 2. Immunoblots were probed with (B) MAb MRPr1 and (C) MAb MRPm6. Arrows denote the position of the full-length MRP1; N1 and N3 denote the long and short NH_2-proximal tryptic fragments, respectively, and C1 and C2 mark the long and short COOH-proximal tryptic fragments, respectively. Similar results were obtained in two additional independent experiments.

as shown previously for the Pro1150Ala mutant (Fig. 2A) [11,13].

3.3. *Ala, Gly, Ile, Leu and Val-substituted mutants of MRP1-Pro^{1150} have similar transport properties*

To determine if the different substitutions of Pro^{1150} affected MRP1 transport activity, ATP-dependent vesicular uptake assays of ^{3}H-labeled LTC_4, $E_2$17βG and MTX were performed. As shown in Fig. 2B–D, the transport properties of all four mutants were similar to that described previously for MRP1-Pro1150Ala [11,13], viz., the mutants exhibited an approximately 50% decrease in LTC_4 transport (Fig. 2B), a 2-fold increase in $E_2$17βG transport (Fig. 2C), and a 3-fold increase in MTX transport (Fig. 2D).

3.4. *Pro^{1150} mutations do not affect substrate binding to MRP1*

To determine whether the decrease in LTC_4 transport by the Pro^{1150} mutants was due to decreased binding of this substrate to MRP1, membrane vesicles were photolabeled with [^{3}H]LTC_4. As observed previously, [^{3}H]LTC_4 photolabeling of the Pro1150Ala mutant was similar to that of wild-type MRP1 (Fig. 3A) [11]. Levels of [^{3}H]LTC_4 labeling of the Pro1150Gly, Pro1150Ile, Pro1150Leu and Pro1150Val mutants were also comparable to wild-type MRP1 (Fig. 3A).

We next examined whether the binding of other MRP1 substrates (e.g. $E_2$17βG and MTX) was affected by Ala substitution of Pro^{1150}. Since photoactive analogs of $E_2$17βG and MTX are not available for direct binding studies, the relative binding affinity of wild-type and mutant MRP1 for these substrates was estimated indirectly by measuring their ability to compete for [^{3}H]LTC_4 photolabeling. As shown in Fig. 3B, $E_2$17βG inhibited [^{3}H]LTC_4 photolabeling of wild-type MRP1 and the MRP1-Pro1150Ala mutant in a comparable concentration dependent fashion. [^{3}H]LTC_4 photolabeling of wild-type and Pro1150Ala mutant MRP1 was also similarly inhibited by MTX (Fig. 3C). These results indicate that binding of LTC_4, $E_2$17βG and MTX to wild-type MRP1 and the MRP1-Pro1150Ala mutant is similar, and thus suggest that the changes observed in the transport of these substrates are not due to changes in their initial binding to MRP1. Comparable experiments were not carried out for the other Pro^{1150} mutants because their transport activities were so similar to those of Pro1150Ala and accordingly, would be expected to exhibit a similar pattern of substrate competition.

3.5. *Mutation of Pro^{1150} does not affect MRP1 sensitivity to chemical modulators*

Because mutation of Pro^{1150} differentially affected the transport of different MRP1 substrates, it was of interest to determine whether the interaction with various MRP1 modulators was also affected. To test this, $E_2$17βG transport by the MRP1-Pro1150Ala mutant was examined in the presence of MK571, S-decyl-GSH, BAY u9773 and LY465803. These four modulators were chosen because of their diverse chemical structures, specificities and modes of inhibitory action. Thus, S-decyl-GSH is a S-alkyl GSH derivative that competitively inhibits MRP1-mediated transport [7]; MK571 does not contain a GSH moiety but is a widely used, but relatively non-specific, inhibitor of MRP1, originally developed as a cysteinyl leukotriene 1 (cysLT1) receptor antagonist [18]; BAY u9773, an inhibitor of MRP1 originally developed as a dual antagonist for cysLT1 and cysLT2 receptors, shares its fatty acid backbone with LTC_4 but is not a GSH conjugate [19] (Nakajima et al., unpublished); and LY465803 is a tricyclic isoxazole derivative which potently inhibits MRP1-mediated transport in a highly specific GSH-dependent manner [14]. As shown in Fig. 4, MK571, S-decyl-GSH, BAY u9773 and LY465803 inhibited MRP1-mediated $E_2$17βG transport with IC_{50} values

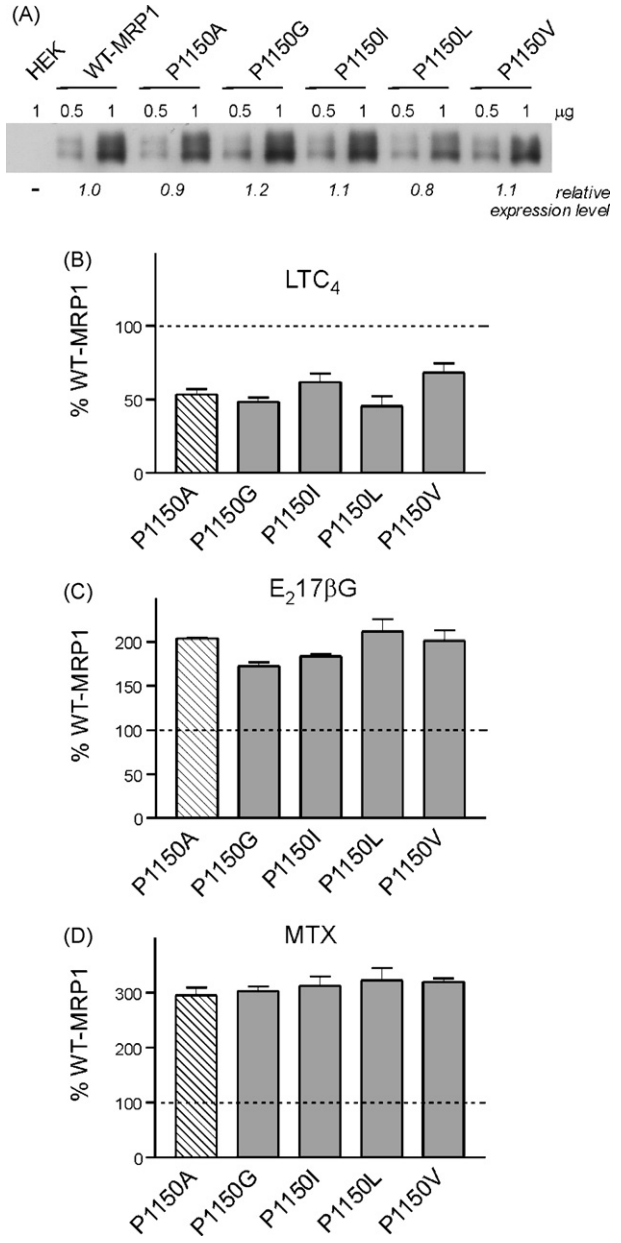

Fig. 2 – Expression and ATP-dependent vesicular transport of ^{3}H-labeled organic anions by MRP1-Pro^{1150} mutants. (A) Membrane vesicles were prepared from HEK293T cells transfected with pcDNA3.1(−)MRP1$_k$ containing Pro^{1150} mutations and protein expression levels were analyzed by immunoblotting. For each sample, 0.5 and 1 μg of membrane protein per lane were resolved by SDS-PAGE and MRP1 detected with MAb QCRL-1. Relative levels of MRP1 were determined by densitometry and are indicated in italics below the blot. HEK refers to vesicles prepared from untransfected HEK293T cells. Similar results were obtained in at least three additional independent experiments, (B) [^{3}H]LTC$_4$ uptake was measured using 2 μg vesicle protein, 50 nM/20 nCi [^{3}H]LTC$_4$ for 1 min at 23 °C, (C) [^{3}H]E$_2$17βG uptake was measured using 2 μg vesicle protein, 400 nM/40 nCi [^{3}H]E$_2$17βG for 1 min at 37 °C and (D) [^{3}H]MTX uptake was measured using 5 μg vesicle protein, 100 μM/250 nCi [^{3}H]MTX for 20 min at 37 °C. Results shown are expressed relative to the transport activity of wild-type MRP1 and are corrected where necessary to take into account differences in protein expression levels of the mutants relative to wild-type MRP1. Bars represent the means (±S.D.) of triplicate determinations in a single experiment; similar results were obtained in at least one additional independent experiment.

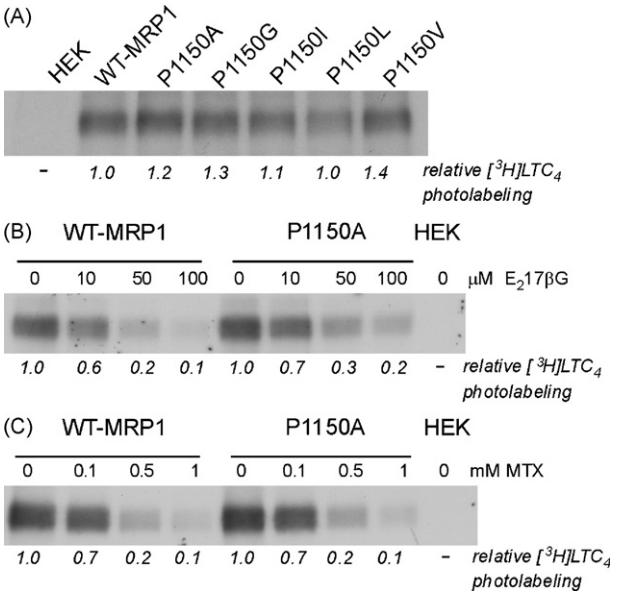

Fig. 3 – Photolabeling of wild-type and Pro^{1150} mutant MRP1 by [^{3}H]LTC$_4$. (A) [^{3}H]LTC$_4$ photolabeling of MRP1-Pro^{1150} mutants was carried out in the absence of organic anion substrates as described in Section 2. Effect of (B) E$_2$17βG and (C) MTX on [^{3}H]LTC$_4$ photolabeling of MRP1. Relative levels of [^{3}H]LTC$_4$ photolabeling are indicated in italics, and where applicable, have been corrected for differences in mutant protein expression compared to wild-type MRP1. HEK refers to control membrane vesicles prepared from untransfected HEK293T cells. Similar results were obtained in one additional independent experiment.

which were similar for both wild-type MRP1 and the MRP1-Pro1150Ala mutant ($p > 0.05$). The effect of the four modulators on E$_2$17βG transport of the other Pro^{1150} mutants was not tested because their transport activities were so similar to those of Pro1150Ala that it would be reasonable to expect them to exhibit similar patterns of inhibitor sensitivity.

3.6. *Pro^{1150} mutants interact similarly with ^{32}P-labeled nucleotide*

We have reported previously that MRP1-Pro1150Ala and wild-type MRP1 bind similar levels of 8N$_3$ATP but vanadate-induced trapping of 8N$_3$ADP by the mutant is greatly reduced [11]. To determine if the other Pro^{1150} mutants exhibited the same characteristics, photolabeling experiments with [^{32}P]8N$_3$ATP under binding (4 °C) and hydrolysis (37 °C) conditions were carried out. As shown in Fig. 5A, the binding of [γ^{32}P]8N$_3$ATP

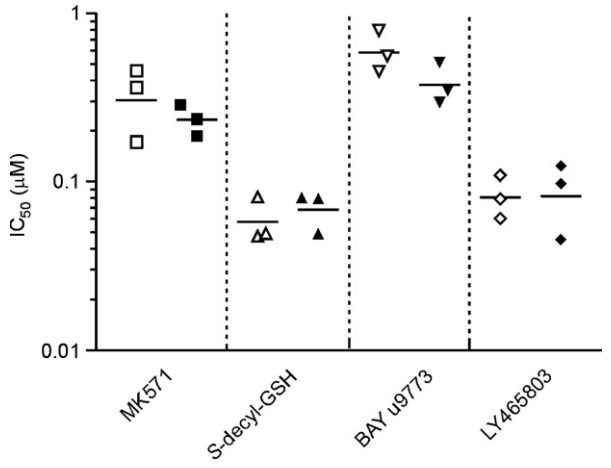

Fig. 4 – Effect of MRP1 modulators on $E_2$17βG transport by wild-type MRP1 and MRP1-Pro1150Ala. [^{3}H]$E_2$17βG uptake was measured with 2 μg protein and 400 nM/40 nCi [^{3}H]$E_2$17βG for 1 min at 37 °C in the presence of multiple concentrations of the indicated modulators and IC_{50} values determined as described in Section 2. Shown on the graphs are the mean IC_{50}'s from three independent experiments. Open symbols represent data obtained with vesicles prepared from cells expressing wild-type MRP1 and filled symbols represent data obtained with vesicles prepared from cells expressing the MRP1-Pro1150Ala mutant. Modulators tested were MK571 (□,■), S-decyl-GSH (△,▲), BAY u9773 (▽,▼) and LY465803 (◇,◆).

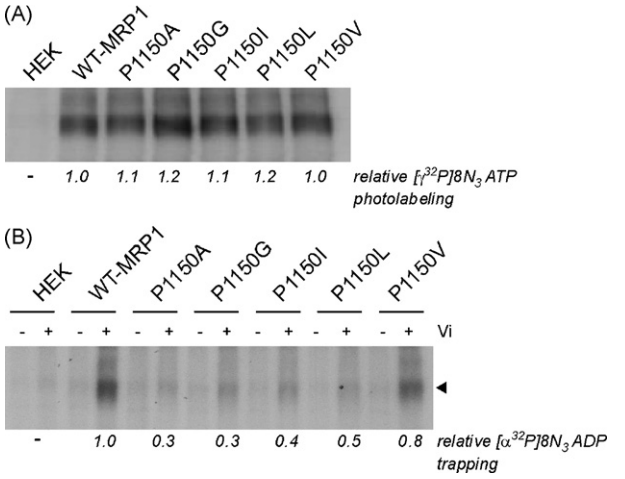

Fig. 5 – Interactions of MRP1-Pro^{1150} mutants with ^{32}P-labeled 8-azidoATP. (A) [γ^{32}P]8N_3ATP photolabeling of wild-type and Pro^{1150} mutants of MRP1. Membrane vesicle protein (10 μg) was incubated with 5 mM $MgCl_2$ and 5 μM [γ^{32}P]8N_3ATP (1 μCi) on ice and then irradiated at 4 °C; labeled proteins were resolved by SDS-PAGE and then exposed to film and (B) vanadate-induced trapping of [α^{32}P]8N_3ADP by wild-type and Pro^{1150} mutants of MRP1. Membrane vesicle protein (10 μg) was incubated with 5 mM $MgCl_2$ and 5 μM [α^{32}P]8N_3ATP (1 μCi) in the presence or absence of 1 mM sodium orthovanadate at 37 °C, washed and irradiated on ice. Samples were then resolved by SDS-PAGE and exposed to film. Films were analyzed by densitometry. Relative levels of [γ^{32}P]8N_3ATP photolabeling and vanadate-induced [α^{32}P]8N_3ADP trapping are indicated in italics and have been corrected, where necessary, for any differences in protein expression levels of the mutants relative to wild-type MRP1. HEK refers to control membrane vesicles prepared from untransfected HEK293T cells.

(5 μM) to MRP1 was not affected by mutation of Pro^{1150} to Gly, Ile, Leu or Val. Even when photolabeling was carried out with a broader range of [γ^{32}P]8N_3ATP concentrations, no differences in photolabeling of the Pro1150Ala mutant and wild-type MRP1 were observed (results not shown).

When nucleotide binding was determined under hydrolysis conditions (37 °C) and in the presence of vanadate, the Pro1150Ala mutant showed a substantial reduction (approximately 70%) in levels of trapped [α^{32}P]8N_3ADP as expected [11]. Under these conditions, the Pro1150Gly, Pro1150Ile and Pro1150Leu mutants exhibited similar levels of [α^{32}P]8N_3ADP trapping (50–70% reduction) (Fig. 5B), while trapping by the Pro1150Val mutant was only slightly reduced (20%) relative to wild-type MRP1 (Fig. 5B).

To exclude the possibility that the decreased vanadate-induced [α^{32}P]8N_3ADP trapping by the MRP1-Pro^{1150} mutants might simply be due to a marked difference in the ability of the mutants to hydrolyze 8N_3ATP versus ATP, the ability of these two nucleotides to support $E_2$17βG uptake into inside-out membrane vesicles was compared. However, as observed when ATP was used, $E_2$17βG uptake by MRP1-Pro1150Ala in the presence of 8N_3ATP was still 2-fold higher than uptake by wild-type MRP1 (results not shown).

To exclude the possibility that diminished interaction between the mutant transporter and vanadate was responsible for the decreased [α^{32}P]8N_3ADP trapping observed, the effect of different concentrations of vanadate on $E_2$17βG transport by the Pro1150Ala mutant was compared with wild-type MRP1. The IC_{50} for vanadate-mediated inhibition of $E_2$17βG transport was ~0.5 mM for wild-type MRP1 and ~1 mM for the Pro1150Ala mutant (results not shown). This relatively modest decrease in the inhibitory potency of vanadate seems unlikely to contribute substantially to the lower level of [α^{32}P]8N_3ADP trapping observed in the MRP1-Pro^{1150} mutants.

3.7. *$E_2$17βG decreases vanadate-induced [α^{32}P]8N_3ADP trapping by wild-type and Pro1150Ala mutant MRP1*

It is generally believed that the presence of substrates can stimulate the ATPase activity of ABC transporters and can thereby enhance levels of vanadate-induced trapping of ADP. Indeed, we and others have shown previously that LTC_4 can stimulate the ATPase activity of purified MRP1 as well as trapping of [α^{32}P]8N_3ADP by wild-type MRP1 although the effect is modest [9,20–23]. Because $E_2$17βG transport by the MRP1-Pro1150Ala mutant was substantially increased, it was of interest to determine if ADP trapping by the wild-type and mutant proteins might be differentially influenced by this substrate. Consequently, [α^{32}P]8N_3ADP trapping experiments with the Pro1150Ala mutant were repeated in the presence of

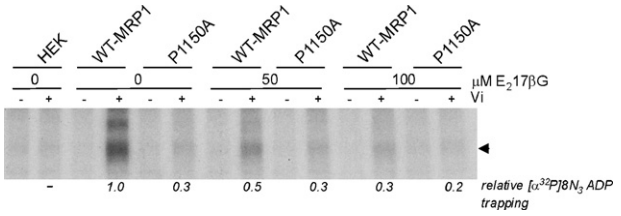

Fig. 6 – Effect of $E_2$17βG on vanadate-induced trapping of [α^{32}P]8N_3ADP by wild-type and Pro1150Ala mutant MRP1. Membrane vesicle protein (10 μg) was preincubated at 4 °C with $E_2$17βG (0, 50, 100 μM) before being processed for vanadate-induced trapping by incubation with 5 mM $MgCl_2$, 5 μM [α^{32}P]8N_3ATP (1 μCi) and sodium orthovanadate (1 mM) at 37 °C as described in the legend to Fig. 5. Relative levels of vanadate-induced [α^{32}P]8N_3ADP trapping are indicated in italics and have been corrected where necessary to take into account differences in expression of the Pro1150Ala mutant relative to wild-type MRP1. HEK refers to control membrane vesicles prepared from untransfected HEK293T cells.

$E_2$17βG. As shown in Fig. 6, $E_2$17βG caused a concentration dependent decrease in trapped [α^{32}P]8N_3ADP by wild-type MRP1 in contrast to the increase observed with LTC_4. Trapping of [α^{32}P]8N_3ADP by the MRP1-Pro1150Ala mutant was also decreased in the presence of $E_2$17βG. Thus both the Pro^{1150} mutation and the presence of $E_2$17βG reduce the vanadate-induced dinucleotide trapping properties of MRP1.

3.8. *Release of 8N_3ADP from MRP1-Pro1150Ala is enhanced relative to wild-type MRP1*

While the decreased trapping of 8N_3ADP by MRP1-Pro1150Ala could be due to reduced ATP hydrolysis, it might also be due to enhanced release of the dinucleotide. To test this latter possibility, trapping conditions were modified to determine if the retention of 8N_3ADP by the transporter (and hence levels of vanadate-induced trapping) could be increased. Thus the temperature at which ATP hydrolysis was carried out was reduced from 37 °C (Fig. 7A, top panel) to 23 °C (Fig. 7A, middle panel). At 23 °C, lower levels of vanadate-trapped [α^{32}P]8N_3ADP by wild-type MRP1 were observed; however, at 37 °C, the amount of [α^{32}P]8N_3ADP trapped by the Pro1150Ala mutant was 40% that of wild-type MRP1 while at 23 °C, the amount trapped increased to 90% of wild-type MRP1.

To determine if the increased trapping of [α^{32}P]8N_3ADP at 23 °C by MRP1-Pro1150Ala was associated with any changes in its transport activity relative to wild-type MRP1, vesicular transport assays were performed at both 23 and 37 °C. As shown in Fig. 7B, $E_2$17βG transport by the Pro1150Ala mutant was 2- to 3-fold higher than wild-type MRP1 at both temperatures. Thus, no differences in relative transport activity were observed at 23 °C despite comparable levels of [α^{32}P]8N_3ADP trapping (and implied ATP hydrolysis) by wild-type and Pro1150Ala mutant MRP1 at this lower temperature.

The possibility that reduced vanadate-induced trapping by MRP1-Pro1150Ala at 37 °C was due to differences in the ability of wild-type MRP1 and MRP1-Pro1150Ala mutant to interact with divalent metal cations was also explored. Thus, Mn^{2+}, Co^{2+}, Ni^{2+}, Zn^{2+} and Cd^{2+} were tested for their ability to support vanadate-induced trapping of [α^{32}P]8N_3ADP by the wild-type and MRP1-Pro1150Ala mutant proteins, and compared to the physiological cation Mg^{2+}. The signal observed with Co^{2+} was 3- and 2.5-fold higher than when using Mn^{2+} and Ni^{2+}, respectively. The signal observed with Mg^{2+} was even lower but could not be compared directly with the signal obtained with Co^{2+} because the Co^{2+} signal was maximal after just 2–3 h film exposure, well before a clear signal for Mg^{2+} could be detected. Zn^{2+} and Cd^{2+} did not support vanadate-induced trapping of 8N_3ADP by MRP1 at all (results not shown). With most divalent cations that supported [α^{32}P]8N_3ADP trapping, the MRP1-Pro1150Ala mutant still trapped significantly less dinucleotide than wild-type MRP1 (≥65% decrease). Interestingly, when Ni^{2+} was used, the difference in trapping levels between the mutant and wild-type MRP1 proteins was reduced, with the trapping signal for MRP1-Pro1150Ala increasing from approximately 40% of wild-type MRP1 in the presence of Mg^{2+} to approximately 70% in the presence of Ni^{2+} (Fig. 7A, bottom panel). $E_2$17βG vesicular uptake measured under these conditions was approximately 20-fold lower in the presence of Ni^{2+} compared to Mg^{2+}, but the >2-fold difference in $E_2$17βG transport activity between wild-type MRP1 and the MRP1-Pro1150Ala mutant was still observed (Fig. 7B).

4. Discussion

In the present study, we have further investigated how substitution of Pro^{1150} alters both the transport and catalytic activities of MRP1 by determining the functional consequences of replacing this residue with a series of amino acids with different physicochemical properties. As a secondary amine, proline is structurally unique among naturally occurring amino acids in that it is the only one with a side chain that cycles back to its backbone. Because its amine group is unavailable for H-bonding, the main-chain interactions that can be crucial for α-helix formation are disrupted and thus proline can cause a kink in an α-helix [24–26]. In addition, the bulky pyrrolidine side chain of proline can introduce conformational constraints that can be important for protein structure and function. Proline residues can also exist in a *cis* or *trans* configuration, a property that may facilitate conformational changes which may take place upon stimulus of a protein such as occurs on substrate or ligand binding, or changes in membrane potential [25,27].

The physicochemical properties of proline can either be conserved or eliminated to varying extents by substitutions with the hydrophobic residues Ala, Leu, Gly, Ile and Val as we have done here. Thus, replacement of Pro^{1150} with alanine is a non-conservative substitution since the small hydrophobic side chain of alanine can support the formation of α-helices although it does not necessarily result in the straightening of the α-helix [26,28,29]. Because of the additional methylene group in its side chain, replacing proline with the bulkier leucine can result in a 'straighter' α-helix than if alanine was present and thus is also a non-conservative substitution [30]. In contrast, substitution of Pro^{1150} with glycine may be considered a conservative substitution because glycine, like

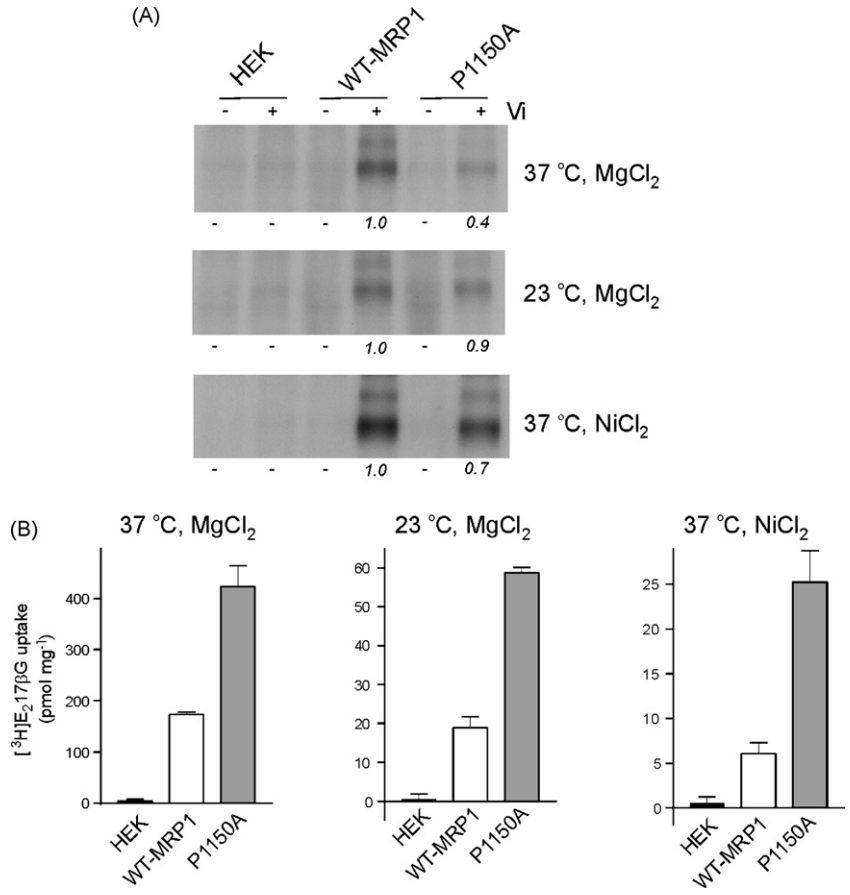

Fig. 7 – Effects of temperature and divalent cations on vanadate-induced [α^{32}P]8N_3ADP trapping and $E_2$17βG transport by wild-type and Pro1150Ala mutant MRP1. (A) Vanadate-induced [α^{32}P]8N_3ADP trapping was performed at 37 °C or 23 °C in the presence of 5 mM $MgCl_2$ or at 37 °C in the presence of 5 mM $NiCl_2$ as indicated. Relative levels of vanadate-induced [α^{32}P]8N_3ADP trapping are indicated in italics and have been corrected where necessary for any differences in mutant protein expression relative to wild-type MRP1. HEK refers to control membrane vesicles prepared from untransfected HEK293T cells and (B) [^{3}H]$E_2$17βG uptake was determined by incubating membrane vesicle protein (2 μg) with 400 nM [^{3}H]$E_2$17βG/40 nCi for 1 min. Uptake was measured at 37 °C or 23 °C and in the presence of 10 mM $MgCl_2$ or $NiCl_2$ as indicated. HEK (black bars), wild-type-MRP1 (open bars) and MRP1-Pro1150Ala (grey bars). Each bar represents the mean (±S.D.) of triplicate determinations from a single experiment; similar results were obtained in one additional independent experiment. Note the different scales on the y-axes.

proline, can disrupt α-helices since its lack of side chain allows it to readily adopt a variety of conformations [28,29]. Replacement of Pro^{1150} with the β-branched amino acids isoleucine and valine may also be viewed as conservative substitutions because like proline, these residues can introduce conformational constraints on α-helices due to the larger space occupied by their side chains [24,31]. Although the tryptic digestion pattern of the Pro1150Ala mutant differed from that of the wild-type protein, indicating that loss of Pro^{1150} does introduce some change in the structure of MRP1, we observed no differences in expression levels of the various MRP1-Pro^{1150} mutants. Thus, despite the differences in the physicochemical properties of the substituting amino acids, any conformational changes they might cause appear insufficient to adversely affect the stability of the transporter.

We also observed that the transport activities of both the conservatively and non-conservatively substituted Pro^{1150} mutants differed from wild-type MRP1 in a similar way. Since none of the hydrophobic amino acids could functionally replace Pro^{1150}, we can conclude that it is the loss of this proline residue rather than the different properties of the substituting amino acids that is responsible for the observed changes in MRP1 function. The similarities of the transport properties of the conservatively and non-conservatively substituted mutants also suggests that it is not simply either the α-helix breaking or the conformation constraining properties of Pro^{1150} that are responsible for the functional importance of this residue.

The [^{3}H]LTC_4 photolabeling studies indicated that the reduced transport of this substrate by the Pro^{1150} mutants is not associated with a substantial change in its binding to MRP1. Similarly, inhibition of [^{3}H]LTC_4 photolabeling by $E_2$17βG and MTX was comparable for the wild-type and MRP1-Pro1150Ala proteins. Therefore, it may be concluded that the substrate selective increases in $E_2$17βG and MTX transport activities are not due to substantial changes in initial

binding of these substrates. Furthermore, despite the marked differences in their chemical structures, specificity and mode of inhibitory action, the unchanged IC_{50} values for the MRP1 modulators MK571, BAY u9773, S-decylGSH and LY465803 also suggest that recognition of these compounds is unaffected by the MRP1-Pro1150Ala mutation.

Although none of the amino acids could replace Pro^{1150} with respect to the substrate specificity of MRP1, it is interesting that MRP1-Pro1150Val exhibited a substantially smaller decrease in vanadate-induced [α^{32}P]8N_3ADP trapping than the other mutants. Thus it appears that the chemical properties of valine allow it to largely replace Pro^{1150} with respect to supporting trapping of [α^{32}P]8N_3ADP by vanadate, but they are unable to restore wild-type substrate specificity. As mentioned earlier, it is well known that the β-branching of the valine side chain, like proline, can introduce conformational constraints on the structure of α-helices [24]. If this is true for the helix extending from TM15 of MRP1 into the cytoplasm, it may be that the constraints caused by valine only partially mimic those present in wild-type MRP1 with proline at position 1150. Further information, which is likely only to be obtained from atomic structures of the transporter, is needed to resolve this issue. For now, it may only be concluded that Pro^{1150} is an important determinant of MRP1 substrate specificity and is also required for efficient vanadate-induced trapping of 8N_3ADP.

Most of the vanadate-induced [α^{32}P]8N_3ADP trapping experiments in this study were performed in the absence of substrate and thus the results obtained are assumed to reflect the basal ATPase activity of MRP1. Previously, we and others have reported that vanadate-induced [α^{32}P]8N_3ADP trapping by MRP1 is modestly increased by LTC_4, an observation interpreted to indicate that this physiological substrate stimulates the ATPase activity of the transporter [9,22,23] which is in accordance with current models that presume that substrate binding initiates the transport cycle of ABC proteins [32]. In contrast to LTC_4, however, we now find that $E_2$17βG decreases [α^{32}P]8N_3ADP trapping by both wild-type MRP1 and the Pro1150Ala mutant. This unexpected observation indicates that somehow, the presence of $E_2$17βG reduces the number of Mg^{2+}·ADP·Vi·MRP1 complexes formed and could imply that unlike LTC_4, $E_2$17βG does not stimulate the ATPase activity of MRP1. Trapping of [α^{32}P]8N_3ADP by the MRP1-Pro1150Ala mutant was also decreased in the presence of $E_2$17βG. Thus both the Pro^{1150} mutation and the presence of $E_2$17βG reduce the dinucleotide trapping properties of MRP1, but whether they do so by precisely the same mechanism remains to be determined. Together these results are consistent with the conclusion that the interactions of $E_2$17βG and LTC_4 with the wild-type protein differ. They also suggest that although both the K_m($E_2$17βG) and K_m(ATP) during $E_2$17βG transport (but not LTC_4 transport) are altered by the Pro^{1150} mutation [11], indicating that the mutant does not interact with $E_2$17βG, or ATP in the presence of $E_2$17βG, in the same way the wild-type protein does, the different interactions are not reflected in substantial differences in initial binding of $E_2$17βG (Fig. 3B).

To explain the decreased vanadate-induced [α^{32}P]8N_3ADP trapping by the MRP1-Pro1150Ala mutant, we hypothesized that rather than decreasing ATP hydrolysis, the mutation was enhancing the release of ADP following ATP hydrolysis, most of which is known to occur at NBD2 [9,33]. It is believed that inorganic phosphate is released first from the NBD and that subsequently, the exogenously added vanadate anion, which structurally mimics the inorganic phosphate, can replace it to form a stable Mg^{2+}·ADP·Vi·MRP1 complex [12,32]. For this to occur, however, the ADP must remain bound long enough to allow the vanadate to move into position and trap it in the transporter. We found that by carrying out the reactions at 23 °C instead of 37 °C (which would presumably increase the occupancy time of 8N_3ADP in NBD2), [α^{32}P]8N_3ADP trapping by MRP1-Pro1150Ala could be increased to levels comparable to that of wild-type MRP1 (Fig. 7). This observation supports the idea that at 37 °C, faster release of ADP from NBD2 of the Pro^{1150} mutant reduces the efficiency with which it can be trapped by vanadate, and hence the level of trapping appears reduced.

To further confirm that the low vanadate-induced 8N_3ADP trapping was due to enhanced release of the dinucleotide, we tried to prolong retention of the nucleotide analog in the NBD by using different divalent metal cations. It has been shown previously that the retention time of ADP in the drug transporting P-glycoprotein differs depending on the cation used [34] and our data suggest that this is also true for MRP1. It is interesting to note that the order of potency with which the bivalent cations support vanadate-induced trapping of [α^{32}P]8N_3ADP ($Co^{2+} > Mn^{2+} = Ni^{2+} > Mg^{2+}$) (Fig. 7 and results not shown) is the inverse of that reported previously for supporting MRP1 transport activity ($Mg^{2+} > Mn^{2+} > Co^{2+}$) [7]. This suggests that cations that increase the retention of ADP in MRP1 (as detected by vanadate trapping) prevent the protein from entering another transport cycle by keeping NBD2 occupied with the hydrolyzed nucleotide.

Although Co^{2+} and Mn^{2+} supported vanadate-induced [α^{32}P]8N_3ADP trapping by wild-type MRP1 to a similar or higher level than Ni^{2+}, they were unable to increase [α^{32}P]8N_3ADP trapping by the MRP1-Pro1150Ala mutant to the same extent as Ni^{2+} (result not shown). It may be that differences in the conformations of the mutant and wild-type MRP1 proteins are responsible for the enhanced release of 8N_3ADP from NBD2, and that Ni^{2+} is the cation that best fits the conformation of the mutant transporter.

Overall, our data clearly indicate that the changes in the transport activities of MRP1-Pro1150Ala and other Pro^{1150} mutants are not tightly linked to the reduced vanadate-induced 8N_3ADP trapping observed. Thus, even when trapping was restored to wild-type or near wild-type levels (as in the case of the valine substitution, or by reducing the temperature or using Ni^{2+}), the transport activities of the MRP1-Pro^{1150} mutants remained significantly different from the wild-type transporter. This is consistent with previously proposed models where ATP-binding is required for substrate transport while ATP hydrolysis and ADP release serves to reset the protein to its native conformation thus allowing a new transport cycle to begin [32,35,36]. This is also consistent with earlier studies that have shown that the binding of ATP is sufficient to decrease the affinity of MRP1 for LTC_4 and estrone sulfate which presumably allows efflux to proceed [33,36,37].

Finally, vanadate-induced trapping experiments are typically carried out in the absence of substrate and therefore do

not strictly represent the ATP hydrolysis occurring during an actual transport cycle, but rather the basal ATPase activity of the transporter. In addition, for reasons that are not yet clear, ADP trapping by several ABC transporters cannot be detected in the presence of the physiological Mg^{2+}cation despite the fact that ATP hydrolysis is clearly occurring [13,38–40]. Thus, while reduced [α^{32}P]8N_3ADP trapping is often interpreted to reflect a decrease in the ability of the transporter to hydrolyze ATP, our data and that of others indicate that such interpretations should be made with some caution because, as demonstrated in the present study, it may instead reflect an enhanced post-hydrolysis release of ADP and reduced occupancy time of the NBD [12].

Lastly, the recently solved high resolution crystal structure of Sav1866, a homodimeric *Staphylococcus aureus* ABC exporter with reasonable homology to MRP1, shows tight interactions between its MSDs and NBDs [35]. There is also evidence that the CLs between the TM helices (referred to as 'coupling helices') are critical conduits for transducing the signals between the NBDs and MSDs that occur during substrate binding and transport [35]. If, as is presumed, MRP1 (and other mammalian ABC exporters) have a structure similar to the Sav1866 homodimer, CL7 where Pro^{1150} and several other mutation-sensitive residues are located [41], could well serve as a coupling helix for interdomain signaling. Nevertheless, precisely how disruption of this loop via loss of Pro^{1150} as shown here, or by mutations of other residues in this region [41], affects both the substrate specificity and catalytic activity of MRP1 (and related ABCC family members) is not known and requires more experimental analysis including high resolution crystal structures of the transporters in the nucleotide and substrate bound states.

Acknowledgments

The authors would like to thank Drs. Gwenaëlle Conseil and Alice Rothnie for helpful discussion and Ms. Kathy Sparks for technical assistance.

REFERENCES

[1] Leslie EM, Deeley RG, Cole SPC. Multidrug resistance proteins: role of P-glycoprotein, MRP1, MRP2, and BCRP (ABCG2) in tissue defense. Toxicol Appl Pharmacol 2005;204:216–37.
[2] Deeley RG, Westlake C, Cole SPC. Transmembrane transport of endo- and xenobiotics by mammalian ATP-binding cassette multidrug resistance proteins. Physiol Rev 2006;86:849–99.
[3] Cole SPC, Bhardwaj G, Gerlach JH, Mackie JE, Grant CE, Almquist KC, et al. Overexpression of a transporter gene in a multidrug-resistant human lung cancer cell line. Science 1992;258:1650–4.
[4] Cole SPC, Sparks KE, Fraser K, Loe DW, Grant CE, Wilson GM, et al. Pharmacological characterization of multidrug resistant MRP-transfected human tumor cells. Cancer Res 1994;54:5902–10.
[5] Morrow CS, Peklak-Scott C, Bishwokarma B, Kute TE, Smitherman PK, Townsend AJ. Multidrug resistance protein 1 (MRP1, ABCC1) mediates resistance to mitoxantrone via glutathione-dependent drug efflux. Mol Pharmacol 2006;69:1499–505.
[6] Loe DW, Almquist KC, Cole SPC, Deeley RG. ATP-dependent 17 β-estradiol 17-(β-D-glucuronide) transport by multidrug resistance protein (MRP) Inhibition by cholestatic steroids. J Biol Chem 1996;271:9683–9.
[7] Loe DW, Almquist KC, Deeley RG, Cole SPC. Multidrug resistance protein (MRP)-mediated transport of leukotriene C_4 and chemotherapeutic agents in membrane vesicles demonstration of glutathione-dependent vincristine transport. J Biol Chem 1996;271:9675–82.
[8] Haimeur A, Conseil G, Deeley RG, Cole SPC. The MRP-related and BCRP/ABCG2 multidrug resistance proteins: biology, substrate specificity and regulation. Curr Drug Metab 2004;5:21–53.
[9] Gao M, Cui HR, Loe DW, Grant CE, Almquist KC, Cole SPC, et al. Comparison of the functional characteristics of the nucleotide binding domains of multidrug resistance protein 1. J Biol Chem 2000;275:13098–108.
[10] Wijnholds J, Evers R, van Leusden MR, Mol CA, Zaman GJ, Mayer U, et al. Increased sensitivity to anticancer drugs and decreased inflammatory response in mice lacking the multidrug resistance-associated protein. Nat Med 1997;3:1275–9.
[11] Koike K, Conseil G, Leslie EM, Deeley RG, Cole SPC. Identification of proline residues in the core cytoplasmic and transmembrane regions of multidrug resistance protein 1 (MRP1/ABCC1) important for transport function, substrate specificity, and nucleotide interactions. J Biol Chem 2004;279:12325–36.
[12] Urbatsch IL, Sankaran B, Bhagat S, Senior AE. Both P-glycoprotein nucleotide-binding sites are catalytically active. J Biol Chem 1995;270:26956–61.
[13] Létourneau IJ, Slot AJ, Deeley RG, Cole SPC. Mutational analysis of a highly conserved proline residue in MRP1, MRP2 and MRP3 reveals a partially conserved function. Drug Metab Dispos 2007;35:1372–9.
[14] Dantzig AH, Shepard RL, Pratt SE, Tabas LB, Lander PA, Ma L, et al. Evaluation of the binding of the tricyclic isoxazole photoaffinity label LY475776 to multidrug resistance associated protein 1 (MRP1) orthologs and several ATP-binding cassette (ABC) drug transporters. Biochem Pharmacol 2004;67:1111–21.
[15] Hipfner DR, Almquist KC, Stride BD, Deeley RG, Cole SPC. Location of a protease-hypersensitive region in the multidrug resistance protein (MRP) by mapping of the epitope of MRP-specific monoclonal antibody QCRL-1. Cancer Res 1996;56:3307–14.
[16] Hipfner DR, Gao M, Scheffer G, Scheper RJ, Deeley RG, Cole SPC. Epitope mapping of monoclonal antibodies specific for the 190-kDa multidrug resistance protein (MRP). Br J Cancer 1998;78:1134–40.
[17] Tabas LB, Dantzig AH. A high-throughput assay for measurement of multidrug resistance protein-mediated transport of leukotriene C_4 into membrane vesicles. Anal Biochem 2002;310:61–6.
[18] Jones TR, Zamboni R, Belley M, Champion E, Charette L, Ford-Hutchinson AW, et al. Pharmacology of L-660, 711 (MK-571): a novel potent and selective leukotriene D_4 receptor antagonist. Can J Physiol Pharmacol 1989;67:17–28.
[19] Tudhope SR, Cuthbert NJ, Abram TS, Jennings MA, Maxey RJ, Thompson AM, et al. BAY u9773, a novel antagonist of cysteinyl-leukotrienes with activity against two receptor subtypes. Eur J Pharmacol 1994;264:317–23.
[20] Chang XB, Hou YX, Riordan JR. ATPase activity of purified multidrug resistance-associated protein. J Biol Chem 1997;272:30962–8.
[21] Mao Q, Leslie EM, Deeley RG, Cole SPC. ATPase activity of purified and reconstituted multidrug resistance protein

MRP1 from drug-selected H69AR cells. Biochim Biophys Acta 1999;1461:69–82.
[22] Bakos E, Evers R, Sinko E, Varadi A, Borst P, Sarkadi B. Interactions of the human multidrug resistance proteins MRP1 and MRP2 with organic anions. Mol Pharmacol 2000;57:760–8.
[23] Leslie EM, Mao Q, Oleschuk CJ, Deeley RG, Cole SPC. Modulation of multidrug resistance protein 1 (MRP1/ABCC1) transport and ATPase activities by interaction with dietary flavonoids. Mol Pharmacol 2001;59:1171–80.
[24] Richardson JS, Richardson DC. Principle and patterns of protein conformation. In: Fasman GD, editor. Prediction of protein structure and the principles of protein conformation. New York: Plenum Press; 1989. p. 1–98.
[25] Deber CM, Therien AG. Putting the β-breaks on membrane protein misfolding. Nat Struct Biol 2002;9:318–9.
[26] von Heijne G. Proline kinks in transmembrane α-helices. J Mol Biol 1991;218:499–503.
[27] Lummis SC, Beene DL, Lee LW, Lester HA, Broadhurst RW, Dougherty DA. *Cis-trans* isomerization at a proline opens the pore of a neurotransmitter-gated ion channel. Nature 2005;438:248–52.
[28] O'Neil KT, DeGrado WF. A thermodynamic scale for the helix-forming tendencies of the commonly occurring amino acids. Science 1990;250:646–51.
[29] Blaber M, Zhang XJ, Matthews BW. Structural basis of amino acid alpha helix propensity. Science 1993;260:1637–40.
[30] Webb DC, Rosenberg H, Cox GB. Mutational analysis of the Escherichia coli phosphate-specific transport system, a member of the traffic ATPase (or ABC) family of membrane transporters A role for proline residues in transmembrane helices. J Biol Chem 1992;267:24661–8.
[31] Petsko GA, Ringe D. Protein structure and function. London: New Science Press Ltd.; 2004.
[32] Higgins CF, Linton KJ. The ATP switch model for ABC transporters. Nat Struct Mol Biol 2004;11:918–26.
[33] Chang XB. A molecular understanding of ATP-dependent solute transport by multidrug resistance-associated protein MRP1. Cancer Metastasis Rev 2007;26:15–37.
[34] Russell PL, Sharom FJ. Conformational and functional characterization of trapped complexes of the *P*-glycoprotein multidrug transporter. Biochem J 2006;399:315–23.
[35] Dawson RJ, Locher KP. Structure of a bacterial multidrug ABC transporter. Nature 2006;443:180–5.
[36] Payen L, Gao M, Westlake C, Theis A, Cole SPC, Deeley RG. Role of carboxylate residues adjacent to the conserved core Walker B motifs in the catalytic cycle of multidrug resistance protein 1 (ABCC1). J Biol Chem 2003;278:38537–4.
[37] Rothnie A, Callaghan R, Deeley RG, Cole SPC. Role of GSH in estrone sulfate binding and translocation by the multidrug resistance protein 1 (MRP1/ABCC1). J Biol Chem 2006;281:13906–14.
[38] Cai J, Daoud R, Alqawi O, Georges E, Pelletier J, Gros P. Nucleotide binding and nucleotide hydrolysis properties of the ABC transporter MRP6 (ABCC6). Biochemistry 2002;41:8058–67.
[39] Ozvegy C, Varadi A, Sarkadi B. Characterization of drug transport, ATP hydrolysis, and nucleotide trapping by the human ABCG2 multidrug transporter modulation of substrate specificity by a point mutation. J Biol Chem 2002;277:47980–9.
[40] Sauna ZE, Nandigama K, Ambudkar SV. Multidrug resistance protein 4 (ABCC4)-mediated ATP hydrolysis: effect of transport substrates and characterization of the post-hydrolysis transition state. J Biol Chem 2004;279:48855–64.
[41] Conseil G, Deeley RG, Cole SPC. Functional importance of three basic residues clustered at the cytosolic interface of transmembrane helix 15 in the multidrug and organic anion transporter MRP1 (ABCC1). J Biol Chem 2006;281.43.50.